ACS OMEGA

http://pubs.acs.org/journal/acsodf

Article

# Porous Silica Biofiber: A Reusable, Sustainable Fertilizer Reservoir

Pulkit Bindra, Mona Nagargade, Bandana Kumari Sahu, Sudhir Kumar Shukla, Ashwini Dutt Pathak, Kamaljit Kaur, Prem Kumar, Sarita Kataria, and Vijayakumar Shanmugam*

Cite This: https://doi.org/10.1021/acsomega.1c05245

Read Online

ACCESS | Metrics & More | Article Recommendations | Supporting Information

**ABSTRACT:** Nitrogen fertilizers, namely urea, are prone to leaching that causes inefficiency in crop production and environmental pollution; hence porous particles were explored for slow release. Nevertheless, discrete particles add cost; therefore, jute cellulose has been tested as twine to tether silica together for reusability. On the other hand, silica serves as an exoskeleton to give pore memory property to cellulose, which otherwise is susceptible to loss of porosity during irrigation. The composite shows ∼70% more absorption capacity in the fifth cycle than the fiber without silica coating. The urea release kinetics shows only <1/3 and 3/4 of urea release from the jute-silica composite compared to naked porous silica and cellulose, respectively. The slow and sustained release of fertilizer from the composite results in a continuous increase in the chlorophyll content in rice crops.

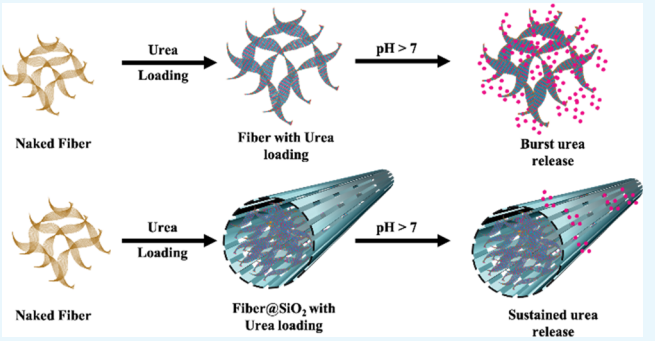




## INTRODUCTION

Nitrogen is one of the essential macronutrients for crop production, which is supplemented through fertilizer application. Among the nitrogen fertilizers, urea contains the highest nitrogen content (∼46%). However, it is prone to leaching and volatilization, significantly reduces its crop uptake efficiency; on the other hand, the loss causes environmental pollution.[1,2] Furthermore, this nitrogen loss is magnified in the acid soil; for instance, it approximates 1−15 kg N loss $ha^{-1}$ $year^{-1}$. Hence, recently attractive nanocomposites were developed to control the fertilizer leaching.[3]

Porous materials have time and again proved efficiency in various applications,[4−7] in which mesoporous silica in drug delivery has gained massive attention in biology.[8] Following this, its role is appreciated in the agricultural formulation that contributed to some of the most refined advanced pesticide delivery formulations.[9−11] Comparatively, its application as a fertilizer reservoir has been limited to diffusion-controlled discrete particles.[12] In this context, we developed an advanced design with mesoporous silica customized to have a biopolymer nanolayer for the targeted fertilizer application.[13] This composite has also controlled the undesired dissipation of the soil solution inside, which otherwise turns fertilizer into an unavailable form.

In mesoporous silica, the feasibility of synthesizing mosaic of architecture like hollow, multishell, yolk−shell, bouquet, branched, dendrimer, and virus-like particles has been demonstrated.[14−16] Considering the feasibility for agricultural application, a composite network is preferred over discrete particles.[17,18] Cellulose, the most abundant biomass on earth, has good mechanical strength, porosity, specific surface area, great functional groups, loading capacity, and so forth, which suits mass-scale application.[19−21] Recently, its compatibility to modify with oxide particles for photothermal applications has been demonstrated.[22] Despite all these desirable properties that can serve as a continuous matrix for the fertilizer reservoir, its poor pore memory property leads to immediate collapse and shrinking in the presence of water. This questions its application in agriculture, where using water during irrigation is unavoidable. Synthesis of silica-based fibrous aerogels with the polymer template has been shown to secure the porosity.[23−27] The combination of cellulose with inorganic and organic supports has been shown to improve flexibility and fiber strength.[28] In such a fertilizer matrix, as much as silica supports the fiber pores, the cellulose running at the core can participate in fluid dynamics control and fertilizer release kinetics in addition to serving as the twine to hold silica for reuse.

Here, a cost-effective cellulose composite with relatively good pore memory property has been prepared with silica coating on a jute template (fiber@$SiO_2$). Jute, a natural polymer with a significant amount of noncellulosic components (up to 40%),[29,30] has poor crystallinity, which is a

Received: September 21, 2021
Accepted: December 22, 2021

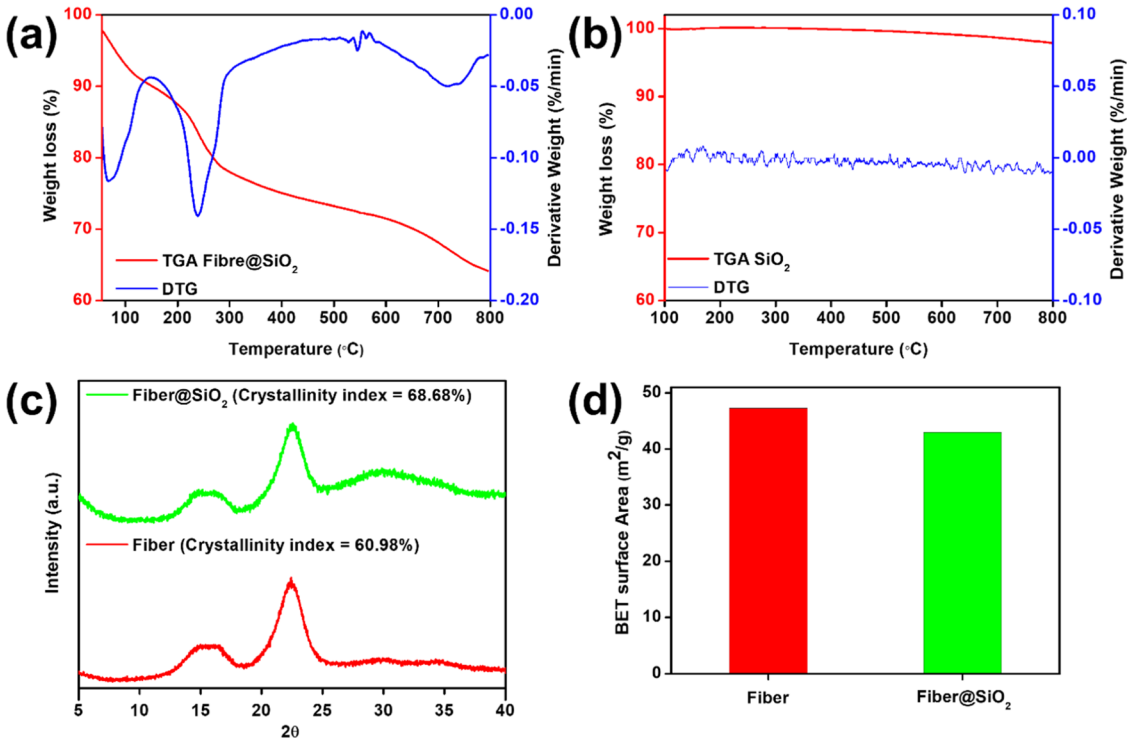


**Figure 1.** Characterization of fiber and fiber@$SiO_2$ starting with TGA and DTG of (a) fiber@$SiO_2$ and (b) $SiO_2$ showing silica quantification, (c) XRD pattern showing the increase in crystallinity after silica coating, and (d) BET surface area showing no significant change in the surface area after silica coating.

favorable property for the porous structure. Compared to other cellulose fibers, the hydrophobicity of jute allows it to remove water from "silica-coated jute" with a minimum collapse in the pore by simple air drying. In contrast, the proper aerogel preparation by silica coating on the hydrophilic polymer template requires freeze or supercritical drying to remove the solvent without a collapse in the pore structure.[31] Thus, the guarantee by the jute for minimum pore collapse in air drying and being the natural fiber ensures environmental compatibility, practical feasibility, and low cost, which qualify to scale up at the industrial level. The regular heterogeneity in the jute having abundant functional groups, aided in the uniform coating that gave good stability to the silica during the mechanical stress test. The porous silica with the fiber template serves as the ultra-lightweight matrix to imbibe ∼12 times the saturated fertilizer volume and show repeated loading/release for multiple cycles. The ability of the fiber to present excellent fluid flow control by running in the porous network channel, enables sustainable fertilizer supply in leach-prone acidic conditions.[32] This release kinetics qualifies the eligibility criteria of European controlled-release fertilizer standards.[33] The composite shows ∼1.25 and 3 times increase in the chlorophyll content in the rice crop on the $10^{th}$ day compared to the urea-loaded fiber and urea treatments, respectively.

## RESULTS AND DISCUSSION

**Material Characterization.** The thermal behavior of the materials was examined through thermogravimetric analysis (TGA) to quantify the amount of silica in fiber@$SiO_2$ (Figure 1a). The initial 12% loss up to 150 °C should be from the removal of moisture content. A subsequent couple of losses, up to 250 °C (15%) and 590 °C (∼3%) may be from hemicellulose and cellulose along with lignin, respectively; whereas in the literature, the cellulose and lignin peaks centered separately at 350 and 500 °C for jute.[34] This shift in fiber@$SiO_2$ may be attributed to the silica coating that caused the coalition of cellulose and lignin decomposition temperature because of silica-confined combustion and carbonation. A similar shift in the cellulose decomposition temperature has been noticed in studies with silica-coated cellulose.[36,37] Compared to the fiber, an additional decomposition peak after 600 °C observed for fiber@$SiO_2$ that corresponds to 7% weight loss, which may account for the carbon loss. Finally, a residual weight corresponding to 62% of the initial weight of the composite was observed at 800 °C. The thermal decomposition of the composite was compared with that of silica, which shows an insignificant loss from the initial weight (Figure 1b). From this, the remaining 62% residual weight from the composite must be the contribution from silica.

Following this, X-ray diffraction (XRD) was recorded to understand the cellulose's crystallinity before and after coating (Figure 1c). Before and after coating, the fiber shows $2\theta$ peaks at 22 and 16°, corresponding to (200) and (110) lattice planes, respectively, confirming the cellulose to be type 1.[38] The crystallinity index calculated shows that the crystallinity improves from 61 to 65% after coating. This minor increase is expected due to the formation of a silica-supported hydrogen bond. This little sacrifice in the amorphous index may not significantly reduce the porosity; however, Brunauer−Emmett−Teller (BET) surface area analysis has been performed to confirm this.

Before and after coating, the fiber has been exposed to the nitrogen adsorption and desorption curve, which shows the surface area to be 47 and 43 $m^2\ g^{-1}$, respectively (Figure 1d). Thus the coating process has not caused significant reduction in the available surface area. This composite is the one with the


https://doi.org/10.1021/acsomega.1c05245
ACS Omega XXXX, XXX, XXX−XXX

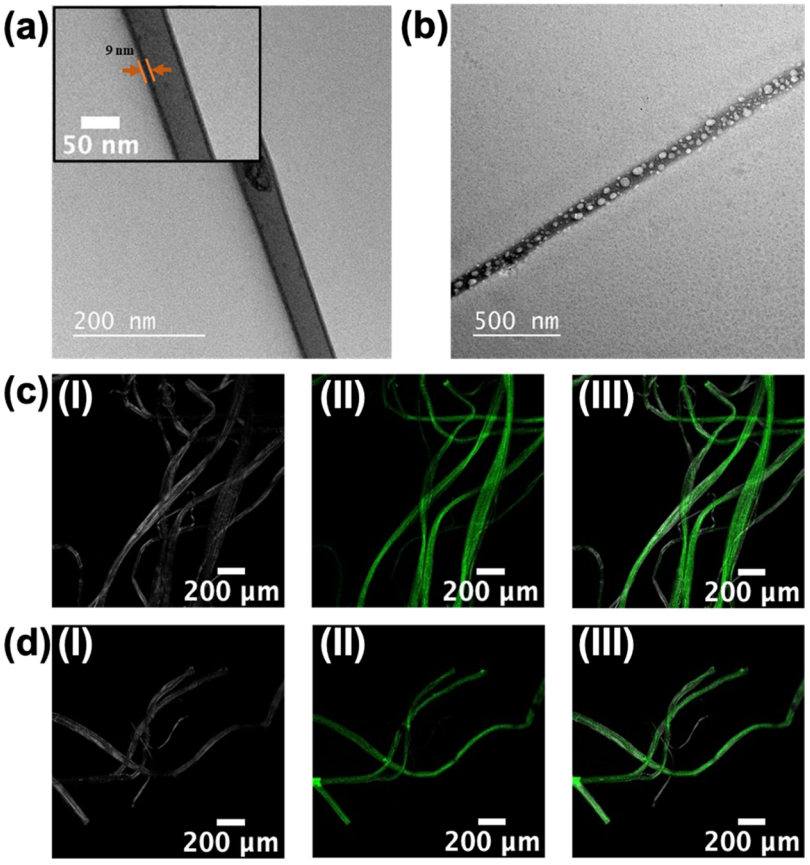


**Figure 2.** TEM micrograph of (a) fiber@$SiO_2$ showing a thick 9 nm silica layer on the fiber (inset) and (b) calcined fiber@$SiO_2$ showing the pores with an average size of 26 nm. (c,d) Confocal fluorescent microscopy image of (c) fiber and (d) fiber@$SiO_2$ (I) darkfield, (II) FITC loaded fiber, and (III) composite image, loaded with FITC. (Using the green channel with a 488 nm laser).

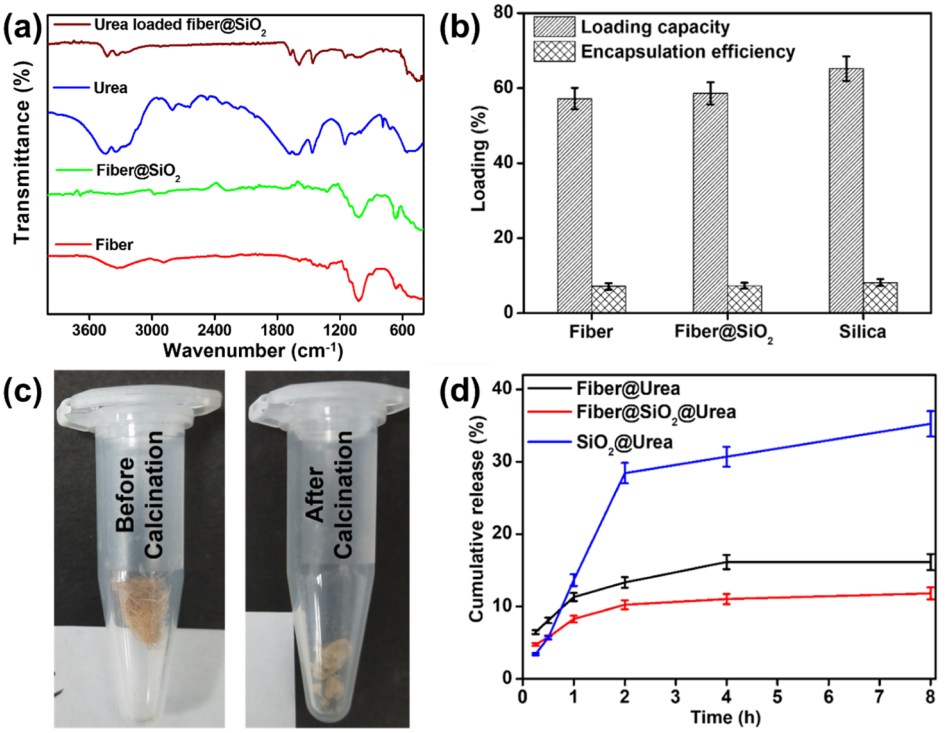


**Figure 3.** (a) FTIR spectra confirming urea loading in the fiber@$SiO_2$ and (b) urea loading and encapsulation efficiency in fiber, fiber@$SiO_2$, and porous silica. (c) Photograph showing the fiber@$SiO_2$ composite before and after calcination and (d) urea release profile from urea-loaded fiber, fiber@$SiO_2$, and porous silica.



https://doi.org/10.1021/acsomega.1c05245
ACS Omega XXXX, XXX, XXX−XXX

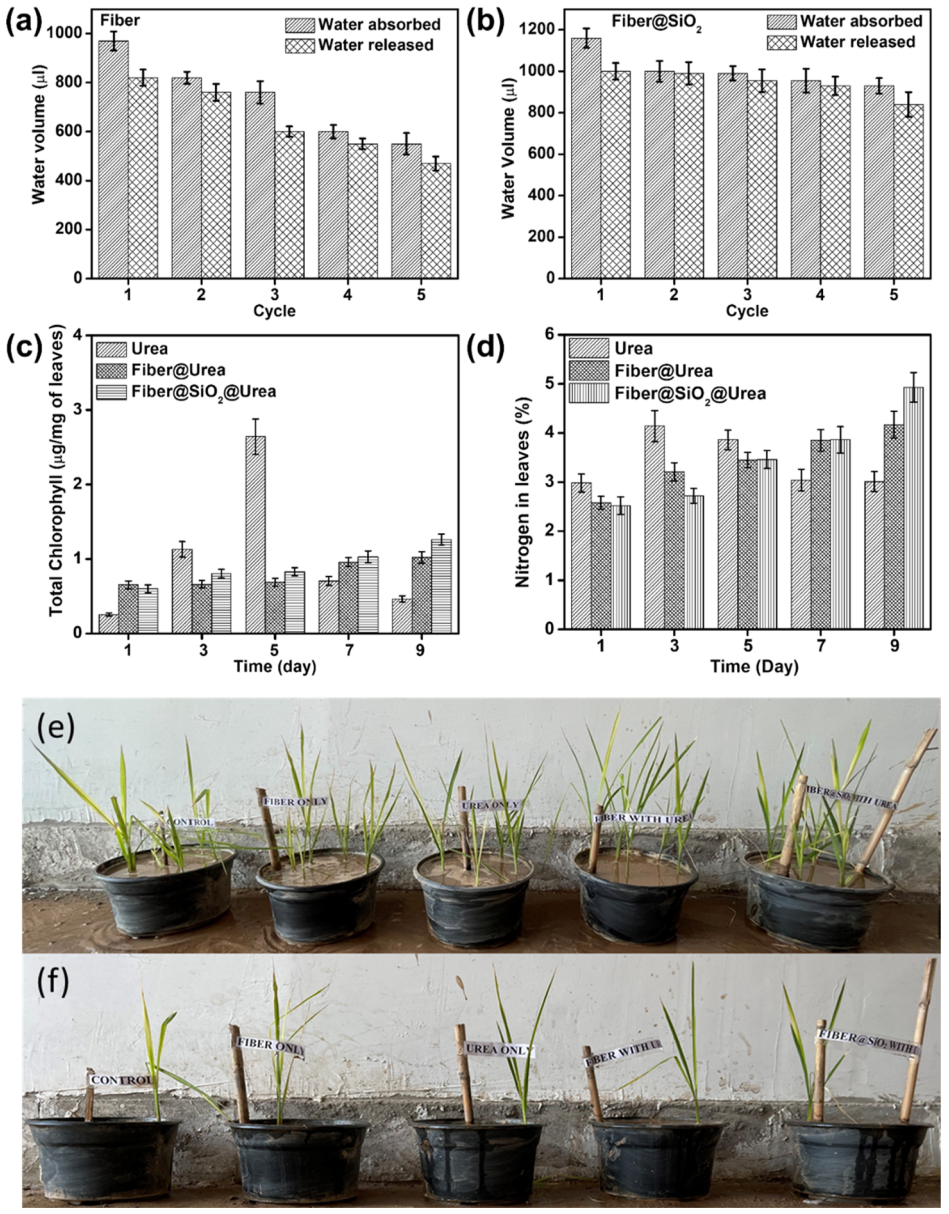


**Figure 4.** (a) Study of absorption capacity and reusability of fiber and (b) fiber@$SiO_2$. (c) Variation in the chlorophyll content in the leaves of rice plants treated with the urea-loaded fiber and urea-loaded composite against a positive control of free urea application. (d) Percentage nitrogen content in the leaves of rice plants treated with the urea-loaded fiber and urea-loaded composite against a positive control of free urea application. (e,f) Photographs showing rice plants in day 1 (e) and day 5 (f) of different treatments.

highest amount of silica (62%), without a significant loss in the surface area [this property has a role in pore recovery (*vide infra*)]. This may be due to the stability offered by the lignin intercalated in the cellulose (jute fiber has the highest amount of lignin in plant cellulose) and is known to provide structural integrity to the plant cell wall.[39] The lignin may have also acted as the reinforcement agent for the fine coating, as previously the organic and inorganic additives were shown to cause integrated growth.[40] Such additives were able to retain the surface area of the fibers even with 60% silica loading.

Before the application, the composite morphology was examined under transmission electron microscopy (TEM) before and after calcination (Figure 2a,b). The image before calcination shows ∼10 nm of thick silica coating on the fiber, which after calcination, shows porous morphology. The appearance of the pore after calcination may be because of the removal of lignin or other nanofiber whiskers that were removed during heating. The pore size varies from 10 to 40 nm in the measured 60 pores, the details of which are given in the Supporting Information (Figure S1 and Table S1). The stability of the silica on the composite has been examined by placing the composite in the drum rotor programmed at 75 rpm for 5 min along with the metal balls. At the end of this stress, no detectable amount of silica was found, which confirms the stability of the silica binding on the fiber.

**Cargo Loading and Release Characterization in Fiber@$SiO_2$.** Before testing the fertilizer loading, the composite was tested for uniform pore access in the mass using fluorescence imaging through the confocal microscope. The images taken for the fibers incubated with the fluorescein isothiocyanate (FITC) before and after silica coating show an even distribution of the green FITC fluorescence with no


https://doi.org/10.1021/acsomega.1c05245
ACS Omega XXXX, XXX, XXX−XXX

difference (Figure 2c,d). This concludes that the silica coating does not restrict the access of the cargo to the fiber, which may be because of the porous nature of the silica coating as observed in the TEM (Figure 2b).

The fiber without and with coating has been allowed to incubate in the saturated urea solution overnight for the fertilizer loading until the equilibrium is reached. Following this, the carriers were washed three times and examined under Fourier transform infrared (FTIR) for loading. The FTIR spectra of the fibers (Figure 3a) show the typical transmittance observed for the jute cellulose at around 2900 and 3300 $cm^{-1}$ corresponding to C−H and O−H stretching.[34] After silica coating on the fiber by the hydrolysis of tetraethoxysilane (TEOS) (fiber@$SiO_2$), the typical Si−O−Si bending vibration peak at 1025−1100 $cm^{-1}$ appears.[35] The narrow ridge at 1170 $cm^{-1}$ observed for the jute broadens and extends till 1250 $cm^{-1}$ after silica coating. An intense peak appears at ∼800 $cm^{-1}$ after silica coating, which corresponds to the Si−O−Si stretching vibrations. The urea-loaded fiber@$SiO_2$ composite shows C−N, C═O stretching, N−H stretching, and N−H deformation at 1453, 1677, 3455, and 1625 $cm^{-1}$, respectively. The urea loading capacity calibrated through the Kjeldahl method shows ∼60% loading in the fiber and fiber@$SiO_2$ (Figure 3b). This phenomenon of even loading in the fiber without and with the coating may be attributed to the reduction in the urea binding site of cellulose by the silica masking being compensated with the gap developed between the fiber and grafted silica wall.

For comparison, a silica control has been synthesized by calcination of fiber@$SiO_2$ in the furnace, so that the fiber has been removed, leaving a white powder (brown composite changed to dirty white) of the porous silica wall (denoted as p1-d$SiO_2$) (Figure 3c). The porous p1-d$SiO_2$ material shows a minor increase in the loading, approximating 5% compared to the fiber and fiber@$SiO_2$. Following this, all the three materials were tested for the release kinetics in the acidic buffer to find the suitability to serve as the fertilizer reservoir in the acid soil, where nitrogen leaching is a severe challenge. Generally, at all observation intervals, the urea release from fiber@$SiO_2$ has been lesser than the fiber and p1-d$SiO_2$ (Figure 3d). In acidic conditions, only <1/3$^{rd}$ of urea has been released from the fiber@$SiO_2$ composite as compared to p1-d$SiO_2$; similarly only 3/4$^{th}$ of urea is released from the fiber@$SiO_2$ composite as compared to cellulose. This controlled release behavior qualifies the fiber@$SiO_2$ composite to be a sustainable fertilizer reservoir in acid soil.

**Absorption Capacity and Reusability Behavior.** For agriculture applications, absorption efficiency and reusability are critical. The fibers with and without silica coating shows total water absorption capacity to be ∼1200 and ∼1000 $\mu$L per 100 mg of jute fiber, respectively (Figure 4a,b). This corresponds to ∼12 and ∼10 times absorption capacity by fiber@$SiO_2$ and fiber, respectively. For the reusability test, the fibers were tested for five cycles of absorption and release; with the application of even pressure on either sides of the glass slides with the samples placed in between. At the end of 5 cycles, the adsorption reduced to 550 $\mu$L in the fiber without coating, whereas the fiber with coating showed 1000 $\mu$L loading at the last cycle too. This indicates that the inorganic silica supports the organic cellulose to regain the porous structure after the compressive stress, which otherwise collapses into the lamellar structure.

To check this phenomenon of the silica support to stabilize the porosity again, we followed the crystallinity of the fiber and fiber@$SiO_2$ exposed to urea loading and washing (Figure S2). Although the initial crystallinity of fiber@$SiO_2$ has been more than the fiber, the crystallinity did not increase after washing, whereas in the fiber, the crystallinity increased by ∼5%. This increase in the crystallinity in the fiber without silica coating can cause loss of porosity, and this phenomenon is explained with the schematic in the Supporting Information (Figure S3). Furthermore, the fiber alone without silica coating does not have the gap; whereas in fiber@$SiO_2$, the silica layer creates gaps between silica and fiber. This gap complements the crystallinity control for the efficient loading in fiber@$SiO_2$.

In addition to converting amorphous cellulose into crystalline, there is also a strong chance for the fiber to swell in the presence of urea, hydrate the NaOH-treated cellulose, and dissolve the amorphous cellulose.[41,42] Eventually, reducing the loading capacity, this phenomenon may be controlled in the silica-coated fiber, namely, fiber@$SiO_2$. Further previous work on aerogel shows the pore recovery property, and it is proportional to the high silica content without the loss of the surface area.[43] This corroborates with fiber@$SiO_2$, which has ∼60% silica with almost no compromise in the surface area.

**Effect of Composites on Plant Physiology.** Nitrogen application is known to affect plant growth directly and chlorophyll content;[44] hence, a pot culture experiment has been performed with the rice crop to assess the efficiency of the composite on the chlorophyll synthesis (Figure 4c). In the control urea application, a sudden increase in the chlorophyll content on the fifth day occurred, which then reduced to less than other treatments in the next couple of days. This may be due to the burst release of nitrogen from the uncoated urea, which is known to cause a sudden increase followed by physiological imbalance. In comparison, the urea application in the fiber and fiber@$SiO_2$ form showed a steady growth for the successive 10 days, which promised a slow and sustained release. The urea-loaded fiber@$SiO_2$ composite shows ∼1.25 and 3 times increase in the chlorophyll content in the rice crop on tenth day compared to the urea-loaded fiber and urea treatments, respectively.

The nitrogen content in plant leaves has been followed for 10 days following the urea application in 23 different forms (1) urea loaded in the fiber, (2) urea loaded in the composite, and (3) free urea application (Figure 4d−f). During the experiment, the pots were irrigated every day with an equal amount of water. In the case of the control plant supplemented with urea, the nitrogen content showed a steep increase at day 3, after which it declined till day 9. This observation correlates with the burst release of nitrogen from the unprotected urea fertilizer. The leaves in the other two treatments, namely, fiber@urea and fiber@$SiO_2$@urea, show a sustainable pattern in the increase of the nitrogen content; thus, although the growth was not as rapid as in the free urea in the initial 3 days, its sustained support led to more nitrogen content than the free urea treatment from seventh day.

Furthermore, at the tenth day, the treatment fiber@$SiO_2$@urea shows significantly more nitrogen than fiber@urea, proving that the silica coating improves the sustainable nitrogen supply to the plant from the fiber. Unlike the fiber treatments where the nitrogen content has shown a continuous increase, there has been a minor fall after the third day in the free urea application, which may be due to the regular heat shock that plants have to overcome after the free urea treatment that leads to nutrient loss. Overall, from this study, it is clear that the fiber@$SiO_2$@urea can contain the fertilizer


https://doi.org/10.1021/acsomega.1c05245
ACS Omega XXXX, XXX, XXX−XXX

over a more extended period with a gradual and sustained release pattern.

## CONCLUSIONS

Cellulose is a low-density high absorptive matrix with good scope to serve as the sustainable fertilizer release matrix. Unfortunately, its inability to retain porosity, which is the key for loading capacity after a cycle, questions the reusability. To maintain the fiber porosity here, porous silica has been grown on natural jute cellulose. The homogeneity with the regular heterogeneity of the small molecules in jute is believed to enable even coating, which ensures the pore retention property to the fiber for multiple cycles with good strength. Furthermore, the silica coating has been optimized in such a way that the coating does not have reduction in the surface area,[36] but still has the ability to retain the porosity after every compression. The urea applied using the fiber@$SiO_2$ composite promised a slow and sustained release of the fertilizer that ensures a continuous increase in the chlorophyll content.

## EXPERIMENTAL DETAILS

**Materials.** TEOS, NaOH, and FITC were purchased from Sigma-Aldrich, India, and all other chemicals used were of analytical grade.

**Fiber Preparation.** Jute fibers were used as the cellulose fiber, and the composition of the fiber includes cellulose (~64%), hemicellulose (~12%), lignin (~12%), wax (0.5%), pectin (0.2%), and water (10%). The fibers were cut to obtain ~5 mm length fibers and washed with water to remove any impurities. The process was repeated three times to remove any visible impurities in the fibers. The water-washed fibers were first dried for 24 h in a hot air oven maintained at 60 °C. The dried fibers were then weighed and treated with NaOH to remove the organic contaminants from the fibers. Briefly, 400 mg of the fiber was placed in 50 mL of 10% NaOH and kept for 2 h under continuous shaking using a magnetic stirrer programmed at 600 rpm. After 2 h, the fibers were washed with type 1 water (Milli-Q water purified using resin filters and deionized using water purification system by millipore systems having very less charge-carrying ions with a specific resistance of 18.2 $\mu\Omega$ and is dispensed through a 0.22 $\mu$m filter) three times to remove any excessive NaOH present. The samples obtained were then kept for drying at 60 °C for 24 h.

**Fiber@$SiO_2$ Composite.** The obtained fibers were coated with silica by using TEOS as the silica precursor. The hydrolysis of TEOS was performed under an alkaline condition in the presence of NaOH. Briefly, 400 mg of fibers and 1.4 mL of NaOH (2 N) were added in 96 mL of type 1 water and incubated at 80 °C for 0.5 h with vigorous stirring. After 0.5 h, 2 mL of TEOS was added into the solution and was kept for another 2 h at 80 °C. The resultant fibers were then washed with water and ethanol (1:1) for 0.2 h at 7000 rpm. The washing was repeated three times, and the obtained samples were dried again at 60 °C for 24 h to remove any water present.

**Characterization of Composite.** Powder XRD analysis was carried out using a Bruker D8 Advance diffractometer. The $N_2$ adsorption−desorption analysis was performed using the Quantachrome instrument Autosorb iQ2 at −196.15 °C. FTIR analysis was performed using a Bruker Vertex 70 series spectrometer with attenuated total reflectance mode. TGA was conducted using PerkinElmer STA 8000. For TEM analysis, samples were suspended in ethanol and drop-coated on a copper grid, followed by drying. The samples were observed under JEOL JEM-2100 (120 kV) for the TEM micrograph. Confocal imaging was carried out using Carl Zeiss LSM, 880 Model equipped with a 488 nm laser line.

**Crystallinity Index Calculation.** The crystallinity index was studied using Ruland's method.[45] In this method, the crystallinity index was calculated by taking the ratio of the crystalline area to the total area using the following equation

$$\text{crystallinity index} = (I_{\text{total}} - I_{\text{am}})/I_{\text{total}}$$

$I_{\text{total}}$ = integrated intensity of the total spectra, $I_{\text{am}}$ = integrated intensity of the amorphous background.

**Loading of FITC in the Composite.** The samples obtained at different stages like the fiber and fiber@$SiO_2$ composite were loaded with FITC. Briefly, for 5 mg of the fiber, 1 mL of FITC solution (50 $\mu$g/mL) was used for loading. The samples were incubated in FITC solution for 24 h, and the samples were washed three times to remove the unbound FITC. The samples obtained were placed on coverslips, covered with glycerol, and viewed under the confocal microscope.

**Loading of Urea in the Composite.** Following the optical confirmation of the cargo loading in fiber@$SiO_2$, urea loading has been quantified. For urea loading in the fiber and fiber@$SiO_2$ composite, initially, a saturated solution of urea (800 mg/mL) was prepared by dissolving urea in type 1 water. Then, 25 mg of the fiber and fiber@$SiO_2$ composite was incubated with 1 mL of the saturated urea solution for 24 h at 400 rpm. The samples were then washed three times with water to remove any unbound-free staying urea on the surface. Loading capacity and encapsulation efficiency were calculated using the formula

$$\text{loading capacity} = [\text{entrapped urea/nanoparticles weight}] \times 100$$

$$\text{encapsulation efficiency} = [(\text{urea added} - \text{unentrapped urea})/\text{urea added}] \times 100$$

**Release of Urea in the Buffer.** Urea-loaded particles with and without silica coating were kept in pH 5 buffer for studying urea release. The composites were incubated in shaking conditions, and samples (20 $\mu$L) were drawn at regular intervals from the supernatant after centrifugation to quantify the released amount. After each sampling, the incubation setup has been filled with the same amount of fresh buffer. The sample so obtained was analyzed using the Kjeldahl method.[46]

**Absorption Capacity and Reusability Behavior.** The reusability of the fiber and fiber@$SiO_2$ was evaluated to check the effect of compression stress on the fibers, especially pore memory and absorption capacity. Equal amounts of fiber and fiber@$SiO_2$ (100 mg each, on a fiber weight basis) were soaked in water to a point where they could not retain more moisture. Uniform pressure was applied on the water-imbibed samples with the glass slides at the end. The amount of water removed was precisely replaced in the next step to maintain the exact volume left by the fiber. These steps were then repeated five times to check the reusability of the fibers.


https://doi.org/10.1021/acsomega.1c05245
ACS Omega XXXX, XXX, XXX−XXX

**Effect of Composite on Plant Physiology.** A pot culture experiment has been conducted to test the impact of the composite on nitrogen supply to the crop. Rice plants (*Oryza sativa*, variety hybrid 103) were transplanted in pots containing 3 kg of soil, in which leaf chlorosis was initiated on 80th day by using water at pH 5 for irrigation. After the onset of chlorosis, the plants were supplemented with external nitrogen in urea, urea loaded inside the fiber and silica-coated fiber. Chlorophyll was extracted and estimated at different time intervals (1, 3, 5, 7, and 9 days).

The spectrophotometry method has been followed for chlorophyll estimation. Briefly, the given leaf weight was ground with 20 mL of acetone (80% aqueous solution prepared in phosphate buffer). The leaves were kept in acetone solution for 24 h at 4 °C with intermittent shaking. Following the incubation, the samples were measured for their absorbance profile through UV−vis spectroscopy against the background signal of acetone solution. The peak values at 645 and 663 nm were used to calculate the chlorophyll content using the following formula.[47]

$$\text{Chlorophyll content} = 20.2(A_{645}) + 8.02(A_{663})$$

## ■ ASSOCIATED CONTENT

### Supporting Information

The Supporting Information is available free of charge at https://pubs.acs.org/doi/10.1021/acsomega.1c05245.

Calculation of pores showing the size distribution of pores in calcined fiber@$SiO_2$ along with the image source, percent crystallinity index change after washing urea-loaded samples in pH 5 buffer in comparison to loaded samples, and schematic representation showing that the presence of silica coating protects the porous structure, and without the silica coating, there is an increase in the crystallinity (PDF)

## ■ AUTHOR INFORMATION


### Corresponding Author

**Vijayakumar Shanmugam** − *Institute of Nano Science and Technology, Mohali, Punjab 140306, India;* orcid.org/0000-0001-7117-5631; Email: vijayakumarshanmugham@gmail.com

### Authors

**Pulkit Bindra** − *Institute of Nano Science and Technology, Mohali, Punjab 140306, India;* orcid.org/0000-0001-6860-5688

**Mona Nagargade** − *Indian Institute of Sugarcane Research, Lucknow 226002, India*

**Bandana Kumari Sahu** − *Institute of Nano Science and Technology, Mohali, Punjab 140306, India*

**Sudhir Kumar Shukla** − *Indian Institute of Sugarcane Research, Lucknow 226002, India*

**Ashwini Dutt Pathak** − *Indian Institute of Sugarcane Research, Lucknow 226002, India*

**Kamaljit Kaur** − *Institute of Nano Science and Technology, Mohali, Punjab 140306, India;* orcid.org/0000-0002-2236-4337

**Prem Kumar** − *Institute of Nano Science and Technology, Mohali, Punjab 140306, India*

**Sarita Kataria** − *Institute of Nano Science and Technology, Mohali, Punjab 140306, India*

Complete contact information is available at: https://pubs.acs.org/10.1021/acsomega.1c05245


### Author Contributions

The manuscript was written through the contributions of all authors. All authors have approved the final version of the manuscript.

### Notes

The authors declare no competing financial interest.

## ■ ACKNOWLEDGMENTS

For financial aid, V.S. thanks the Department of Science and Technology-Science and Engineering Research Board (DST-SERB), Government of India (CRG/2019/006317). The authors are thankful to the Institute of Nano Science and Technology for the funding support.

## ■ REFERENCES


(1) Singh, R.; Kirk, G. J. D. A Model for Predicting the Fate of Nitrogen Fertilizer in Lowland Ricefields. *J. Soil Sci.* **1993**, *44*, 271−283.

(2) Leviel, B.; Gabrielle, B.; Justes, E.; Mary, B.; Gosse, G. Water and Nitrate Budgets in a Rendzina Cropped with Oilseed Rape Receiving Varying Amounts of Fertilizer. *Eur. J. Soil Sci.* **1998**, *49*, 37−51.

(3) Barbi, S.; Barbieri, F.; Andreola, F.; Lancellotti, I.; Barbieri, L.; Montorsi, M. Preliminary Study on Sustainable NPK Slow-Release Fertilizers Based on Byproducts and Leftovers: A Design-of-Experiment Approach. *ACS Omega* **2020**, *5*, 27154−27163.

(4) Lian, Z.; Wang, W.; Li, G.; Tian, F.; Schanze, K. S.; Li, H. Pt-Enhanced Mesoporous Ti3+/TiO2 with Rapid Bulk to Surface Electron Transfer for Photocatalytic Hydrogen Evolution. *ACS Appl. Mater. Interfaces* **2017**, *9*, 16959−16966.

(5) Tian, W.; Lin, J.; Zhang, H.; Duan, X.; Sun, H.; Wang, H.; Wang, S. Enhanced Removals of Micropollutants in Binary Organic Systems by Biomass Derived Porous Carbon/Peroxymonosulfate. *J. Hazard. Mater.* **2021**, *408*, 124459.

(6) Sharma, S.; Sahu, B. K.; Cao, L.; Bindra, P.; Kaur, K.; Chandel, M.; Koratkar, N.; Huang, Q.; Shanmugam, V. Porous nanomaterials: Main vein of agricultural nanotechnology. *Prog. Mater. Sci.* **2021**, *121*, 100812.

(7) Kumar, V.; Alwekar, S. P.; Kunc, V.; Cakmak, E.; Kishore, V.; Smith, T.; Lindahl, J.; Vaidya, U.; Blue, C.; Theodore, M.; Kim, S.; Hassen, A. A. High-Performance Molded Composites Using Additively Manufactured Preforms with Controlled Fiber and Pore Morphology. *Addit. Manuf.* **2021**, *37*, 101733.

(8) Chen, W.; Glackin, C. A.; Horwitz, M. A.; Zink, J. I. Nanomachines and Other Caps on Mesoporous Silica Nanoparticles for Drug Delivery. *Acc. Chem. Res.* **2019**, *52*, 1531−1542.

(9) Zhang, W.; He, S.; Liu, Y.; Geng, Q.; Ding, G.; Guo, M.; Deng, Y.; Zhu, J.; Li, J.; Cao, Y. Preparation and Characterization of Novel Functionalized Prochloraz Microcapsules Using Silica-Alginate-Elements as Controlled Release Carrier Materials. *ACS Appl. Mater. Interfaces* **2014**, *6*, 11783−11790.

(10) Kaziem, A. E.; Gao, Y.; He, S.; Li, J. Synthesis and Insecticidal Activity of Enzyme-Triggered Functionalized Hollow Mesoporous Silica for Controlled Release. *J. Agric. Food Chem.* **2017**, *65*, 7854−7864.

(11) Gao, Y.; Zhang, Y.; He, S.; Xiao, Y.; Qin, X.; Zhang, Y.; Li, D.; Ma, H.; You, H.; Li, J. Fabrication of a Hollow Mesoporous Silica Hybrid to Improve the Targeting of a Pesticide. *Chem. Eng. J.* **2019**, *364*, 361−369.

(12) Wanyika, H.; Gatebe, E.; Kioni, P.; Tang, Z.; Gao, Y. Mesoporous Silica Nanoparticles Carrier for Urea: Potential Applications in Agrochemical Delivery Systems. *J. Nanosci. Nanotechnol.* **2012**, *12*, 2221−2228.

(13) Bindra, P.; Kaur, K.; Rawat, A.; De Sarkar, A.; Singh, M.; Shanmugam, V. Nano-Hives for Plant Stimuli Controlled Targeted Iron Fertilizer Application. *Chem. Eng. J.* **2019**, *375*, 121995.
(14) Zhao, T.; Chen, L.; Lin, R.; Zhang, P.; Lan, K.; Zhang, W.; Li, X.; Zhao, D. Interfacial Assembly Directed Unique Mesoporous Architectures: From Symmetric to Asymmetric. *Acc. Mater. Res.* **2020**, *1*, 100−114.
(15) Qiu, P.; Ma, B.; Hung, C.-T.; Li, W.; Zhao, D. Spherical Mesoporous Materials from Single to Multilevel Architectures. *Acc. Chem. Res.* **2019**, *52*, 2928−2938.
(16) Peng, L.; Hung, C.-T.; Wang, S.; Zhang, X.; Zhu, X.; Zhao, Z.; Wang, C.; Tang, Y.; Li, W.; Zhao, D. Versatile Nanoemulsion Assembly Approach to Synthesize Functional Mesoporous Carbon Nanospheres with Tunable Pore Sizes and Architectures. *J. Am. Chem. Soc.* **2019**, *141*, 7073−7080.
(17) Zhou, L.; Zhao, P.; Chi, Y.; Wang, D.; Wang, P.; Liu, N.; Cai, D.; Wu, Z.; Zhong, N. Controlling the Hydrolysis and Loss of Nitrogen Fertilizer (Urea) by Using a Nanocomposite Favors Plant Growth. *ChemSusChem* **2017**, *10*, 2068−2079.
(18) Zhou, L.; Cai, D.; He, L.; Zhong, N.; Yu, M.; Zhang, X.; Wu, Z. Fabrication of a High-Performance Fertilizer to Control the Loss of Water and Nutrient Using Micro/Nano Networks. *ACS Sustainable Chem. Eng.* **2015**, *3*, 645−653.
(19) Ashokkumar, M.; Thanikaivelan, P.; Krishnaraj, K.; Chandrasekaran, B. Transforming Chromium Containing Collagen Wastes into Flexible Composite Sheets Using Cellulose Derivatives: Structural, Thermal, and Mechanical Investigations. *Polym. Compos.* **2011**, *32*, 1009−1017.
(20) Sobhanadhas, L. S.; Kesavan, L.; Lastusaari, M.; Fardim, P. Layered Double Hydroxide-Cellulose Hybrid Beads: A Novel Catalyst for Topochemical Grafting of Pulp Fibers. *ACS Omega* **2019**, *4*, 320−330.
(21) Li, H.; Wang, C.; Xu, Y.; Yu, Z.; Saravanamurugan, S.; Wu, Z.; Yang, S.; Luque, R. Heterogeneous (de)Chlorination-Enabled Control of Reactivity in the Liquid-Phase Synthesis of Furanic Biofuel from Cellulosic Feedstock. *Green Chem.* **2020**, *22*, 637−645.
(22) Han, S.; Han, K.; Hong, J.; Yoon, D.-Y.; Park, C.; Kim, Y. Photothermal Cellulose-Patch with Gold-Spiked Silica Microrods Based on Escherichia coli. *ACS Omega* **2018**, *3*, 5244−5251.
(23) Meador, M. A. B.; Capadona, L. A.; McCorkle, L.; Papadopoulos, D. S.; Leventis, N. Structure-Property Relationships in Porous 3D Nanostructures as a Function of Preparation Conditions: Isocyanate Cross-Linked Silica Aerogels. *Chem. Mater.* **2007**, *19*, 2247−2260.
(24) Meador, M. A. B.; Weber, A. S.; Hindi, A.; Naumenko, M.; McCorkle, L.; Quade, D.; Vivod, S. L.; Gould, G. L.; White, S.; Deshpande, K. Structure-Property Relationships in Porous 3D Nanostructures: Epoxy-Cross-Linked Silica Aerogels Produced Using Ethanol as the solvent. *ACS Appl. Mater. Interfaces* **2009**, *1*, 894−906.
(25) Nguyen, B. N.; Meador, M. A. B.; Tousley, M. E.; Shonkwiler, B.; McCorkle, L.; Scheiman, D. A.; Palczer, A. Tailoring Elastic Properties of Silica Aerogels Cross-Linked with Polystyrene. *ACS Appl. Mater. Interfaces* **2009**, *1*, 621−630.
(26) Capadona, L. A.; Meador, M. A. B.; Alunni, A.; Fabrizio, E. F.; Vassilaras, P.; Leventis, N. Flexible, Low-Density Polymer Crosslinked Silica Aerogels. *Polymer* **2006**, *47*, 5754−5761.
(27) Tripathi, A.; Parsons, G. N.; Rojas, O. J.; Khan, S. A. Featherlight, Mechanically Robust Cellulose Ester Aerogels for Environmental Remediation. *ACS Omega* **2017**, *2*, 4297−4305.
(28) Fu, B.; Yang, Q.; Yang, F. Flexible Underwater Oleophobic Cellulose Aerogels for Efficient Oil/Water Separation. *ACS Omega* **2020**, *5*, 8181−8187.
(29) Khan, F.; Ahmad, S. R.; Kronfli, E. γ-Radiation Induced Changes in the Physical and Chemical Properties of Lignocellulose. *Biomacromolecules* **2006**, *7*, 2303−2309.
(30) Magniez, K.; Voda, A. S.; Kafi, A. A.; Fichini, A.; Guo, Q.; Fox, B. L. Overcoming Interfacial Affinity Issues in Natural Fiber Reinforced Polylactide Biocomposites by Surface Adsorption of Amphiphilic Block Copolymers. *ACS Appl. Mater. Interfaces* **2013**, *5*, 276−283.
(31) Leventis, N. Three-Dimensional Core-Shell Superstructures: Mechanically Strong Aerogels. *Acc. Chem. Res.* **2007**, *40*, 874−884.
(32) Jiang, N.; Li, Y.; Li, D.; Yu, T.; Li, Y.; Xu, J.; Li, N.; Marrow, T. J. 3D Finite Element Modeling of Water Diffusion Behavior of Jute/PLA Composite Based on X-Ray Computed Tomography. *Compos. Sci. Technol.* **2020**, *199*, 108313.
(33) *Slow-Release Fertilizers—Determination of the Release of the Nutrients—Method for Coated Fertilizers*; Switzerland, 2017. ISO 21263.
(34) Sharma, P. R.; Joshi, R.; Sharma, S. K.; Hsiao, B. S. A Simple Approach to Prepare Carboxycellulose Nanofibers from Untreated Biomass. *Biomacromolecules* **2017**, *18*, 2333−2342.
(35) Pirzada, T.; Ashrafi, Z.; Xie, W.; Khan, S. A. Cellulose Silica Hybrid Nanofiber Aerogels: From Sol−Gel Electrospun Nanofibers to Multifunctional Aerogels. *Adv. Funct. Mater.* **2020**, *30*, 1907359.
(36) Sai, H.; Fu, R.; Xing, L.; Xiang, J.; Li, Z.; Li, F.; Zhang, T. Surface Modification of Bacterial Cellulose Aerogels' Web-like Skeleton for Oil/Water Separation. *ACS Appl. Mater. Interfaces* **2015**, *7*, 7373−7381.
(37) Litschauer, M.; Neouze, M.-A.; Haimer, E.; Henniges, U.; Potthast, A.; Rosenau, T.; Liebner, F. Silica Modified Cellulosic Aerogels. *Cellulose* **2011**, *18*, 143−149.
(38) Smith, C. J.; Wagle, D. V.; Bhawawet, N.; Gehrke, S.; Hollóczki, O.; Pingali, S. V.; O'Neill, H.; Baker, G. A. Combined Small-Angle Neutron Scattering, Diffusion NMR, and Molecular Dynamics Study of a Eutectogel: Illuminating the Dynamical Behavior of Glyceline Confined in Bacterial Cellulose Gels. *J. Phys. Chem. B* **2020**, *124*, 7647−7658.
(39) Vermaas, J. V.; Crowley, M. F.; Beckham, G. T. A Quantitative Molecular Atlas for Interactions between Lignin and Cellulose. *ACS Sustainable Chem. Eng.* **2019**, *7*, 19570−19583.
(40) Cai, J.; Liu, S.; Feng, J.; Kimura, S.; Wada, M.; Kuga, S.; Zhang, L. Cellulose-Silica Nanocomposite Aerogels by InSituFormation of Silica in Cellulose Gel. *Angew. Chem., Int. Ed.* **2012**, *51*, 2076−2079.
(41) Rol, F.; Sillard, C.; Bardet, M.; Yarava, J. R.; Emsley, L.; Gablin, C.; Léonard, D.; Belgacem, N.; Bras, J. Cellulose Phosphorylation Comparison and Analysis of Phosphorate Position on Cellulose Fibers. *Carbohydr. Polym.* **2020**, *229*, 115294.
(42) Gunnarsson, M.; Bernin, D.; Hasani, M. On the Interference of Urea with CO2/CO32- Chemistry of Cellulose Model Solutions in NaOH(Aq). *Carbohydr. Polym.* **2021**, *251*, 117059.
(43) Zhang, Z.; Sèbe, G.; Rentsch, D.; Zimmermann, T.; Tingaut, P. Ultralightweight and Flexible Silylated Nanocellulose Sponges for the Selective Removal of Oil from Water. *Chem. Mater.* **2014**, *26*, 2659−2668.
(44) Kawakami, E. M.; Oosterhuis, D. M.; Snider, J. L. Nitrogen Assimilation and Growth of Cotton Seedlings under NaCl Salinity and in Response to Urea Application with NBPT and DCD. *J. Agron. Crop Sci.* **2013**, *199*, 106−117.
(45) Ruland, W. X-Ray Determination of Crystallinity and Diffuse Disorder Scattering. *Acta Crystallogr.* **1961**, *14*, 1180−1185.
(46) Humphries, E. C. Mineral Components and Ash Analysis. *Modern Methods of Plant Analysis*; Springer: Berlin, Heidelberg, 1956; pp 468−502.
(47) Sharma, S.; Sahu, B.; Srinivasan, S.; Singh, M.; Govindasamy, J.; Shanmugam, V. Effect of Galvanotaxis Graphene Oxide on Chloroplast Activity: Interaction Quantified with Biolayer-Interferometry Coupled Confocal Microscopy. *Carbon* **2020**, *162*, 147−156.


https://doi.org/10.1021/acsomega.1c05245
*ACS Omega* XXXX, XXX, XXX−XXX